

## Spontaneous fission properties of 2.9-s $^{256}\text{No}$

D. C. Hoffman, D. M. Lee, K. E. Gregorich, M. J. Nurmia, R. B. Chadwick, K. B. Chen,\*  
 K. R. Czerwinski, C. M. Gannett, H. L. Hall, R. A. Henderson, B. Kadkhodayan, S. A. Kreek, and J. D. Leyba  
*Nuclear Science Division, Lawrence Berkeley Laboratory, Berkeley, California 94720*  
*and Chemistry Department, University of California, Berkeley, Berkeley, California 94720*

(Received 5 October 1989)

We have measured the mass and kinetic-energy distributions of fragments from the spontaneous fission of  $^{256}\text{No}$  produced via the  $^{248}\text{Cm}(^{12}\text{C},4n)$  reaction. The production cross section using 71-MeV  $^{12}\text{C}$  projectiles was found to be 250 nb. The total kinetic energy for spontaneous fission of  $^{256}\text{No}$  is  $196 \pm 3$  MeV. The mass distribution is very broad (full width at half maximum of  $\sim 50$  mass units) with no appreciable decrease in yield for symmetric mass division.  $^{256}\text{No}$  seems to be the transition nucleus between the asymmetric mass division observed for spontaneous fission of the lighter No isotopes and the symmetric mass division observed for the heavier No isotopes. Its properties are similar to those of  $^{257}\text{Fm}$ , the isotope at which this transition occurs in the Fm isotopes, but the  $^{256}\text{No}$  mass distribution is broader than that for  $^{257}\text{Fm}$ , and its average total kinetic energy for symmetric mass division is about 15 MeV lower. We determined the half-life of  $^{256}\text{No}$  to be  $2.91 \pm 0.05$  s by measuring its  $\alpha$  decay. We measured a spontaneous fission to  $\alpha$  ratio of  $0.0053^{+0.0006}_{-0.0003}$ , which gives a partial half-life for spontaneous fission of  $550^{+40}_{-70}$  s. An energy of  $8.448 \pm 0.006$  MeV was measured for the  $\alpha$ -particle decay to the ground state of  $^{252}\text{Fm}$ , allowing us to calculate the mass excess for  $^{256}\text{No}$  as  $87820 \pm 8$  keV. The energy of the  $2^+$  rotational level in the  $^{252}\text{Fm}$  daughter is  $47 \pm 5$  keV, and the intensity of the 8.402-MeV  $\alpha$  group populating this level is  $(13 \pm 2)\%$ .

### I. INTRODUCTION

Studies of the spontaneous fission (SF) properties of heavy actinide nuclides in the region of Fm ( $Z = 100$ ) are of particular interest because of the sudden transition from the asymmetric mass division observed in the SF of all the lighter actinides to the very symmetric mass division accompanied by anomalously high total kinetic energy (TKE) found in SF of the heavier Fm isotopes. This transition was first found<sup>1</sup> to occur in Fm between  $^{256}\text{Fm}$  and  $^{258}\text{Fm}$ ,  $^{257}\text{Fm}$  being a transition nucleus with much enhanced yields and high TKE's for symmetric mass division. Mass-yield and kinetic-energy distributions have now been measured for seven isotopes of Fm, the lightest being  $^{246}\text{Fm}$  and the heaviest  $^{259}\text{Fm}$ . The transition from asymmetric to symmetric mass division for the Fm isotopes is shown schematically in Fig. 1, together with mass-yield curves for SF of other trans-Bk isotopes. Double-humped mass-yield distributions, typical of the asymmetric mass division of the low-energy and spontaneous fission of the lighter actinides, and TKE's consistent with the linear function of  $Z^2/A^{1/3}$  (Fig. 2) obtained for the lower  $Z$  actinides are observed up through  $^{256}\text{Fm}$ . However,  $^{257}\text{Fm}$  shows a large increase in the yield of symmetric mass division, and symmetric mass division with very high TKE becomes the most probable mode for  $^{258}\text{Fm}$  and  $^{259}\text{Fm}$ . With the recent measurements<sup>7</sup> of  $^{262}\text{No}$ , the most neutron-rich nuclide so far identified, information for three No isotopes is available and a transition (see Fig. 1) similar to that observed for the Fm isotopes is seen:  $^{252}\text{No}$  shows an asymmetric mass distribution with "normal" TKE;  $^{258}\text{No}$

shows predominantly symmetric mass division with near normal TKE, but with some evidence for a higher energy component;  $^{262}\text{No}$  shows a narrowly symmetric mass-yield distribution with high TKE, but with some evidence for a component with lower TKE. The TKE distributions for  $^{258}\text{No}$  and  $^{262}\text{No}$ , together with those for some other heavy trans-Es isotopes, are shown schematically in Fig. 3.

As can be seen in Fig. 1, the transition from asymmetric to symmetric mass division in the No isotopes must take place somewhere between  $N = 150$  and  $N = 156$ , apparently at a somewhat smaller neutron number than in the Fm isotopes. Thus it is of interest to examine the fission properties of  $^{256}\text{No}$  ( $N = 154$ ) to determine whether it is indeed a "transition" nucleus similar to  $^{257}\text{Fm}$  ( $N = 157$ ).

Ghiorso *et al.*<sup>8</sup> produced  $^{256}\text{No}$  using the  $^{248}\text{Cm}(^{12}\text{C},4n)$ ,  $^{248}\text{Cm}(^{13}\text{C},5n)$ , and  $^{246}\text{Cm}(^{13}\text{C},3n)$  reactions with cross sections of 0.74, 0.75, and 0.09  $\mu\text{b}$ , respectively. They measured 8.43  $\pm$  0.02-MeV  $\alpha$  particles in all three reactions and obtained  $\alpha$  half-lives of  $2.9 \pm 0.5$  and  $3.2 \pm 0.2$  s in the first two reactions, respectively. They estimated the SF/ $\alpha$  ratio to be  $\sim 1/400$  in the first reaction although they indicated that the mass assignment of the SF activity was not conclusive. Flerov *et al.*<sup>9</sup> produced a  $3.7 \pm 0.5$ -s, 8.43  $\pm$  0.03-MeV  $\alpha$  activity in the  $^{242}\text{Pu}(^{18}\text{O},4n)$  and  $^{238}\text{U}(^{22}\text{Ne},4n)$  reactions and attributed it to  $^{256}\text{No}$ , but stated that they regarded their previous measurement of the partial SF half-life of  $\sim 1500$  s as only a lower limit.

We have used the  $^{248}\text{Cm}(^{12}\text{C},4n)$  reaction to produce  $^{256}\text{No}$  and have measured the SF-to-alpha ratio, the  $\alpha$

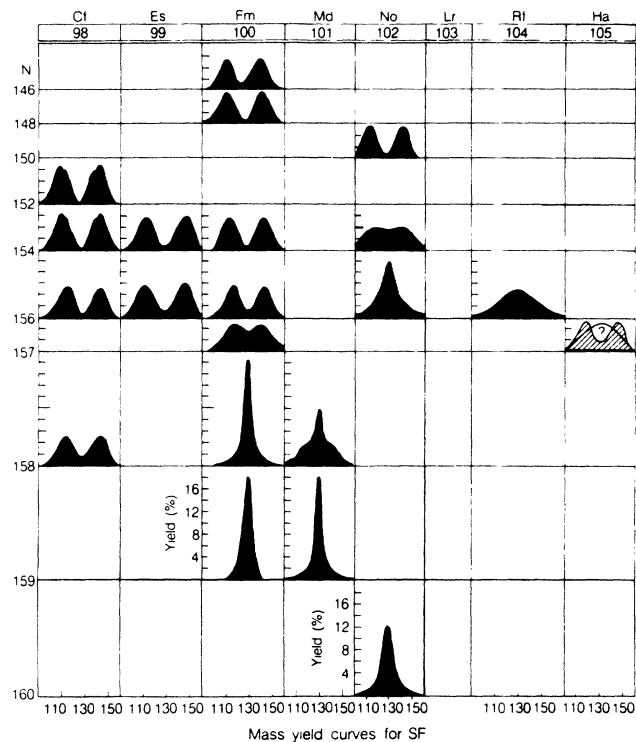


FIG. 1. Schematic of mass-yield distributions, normalized to 200% fission fragment yield, for SF of trans-Bk isotopes (from Ref. 2).

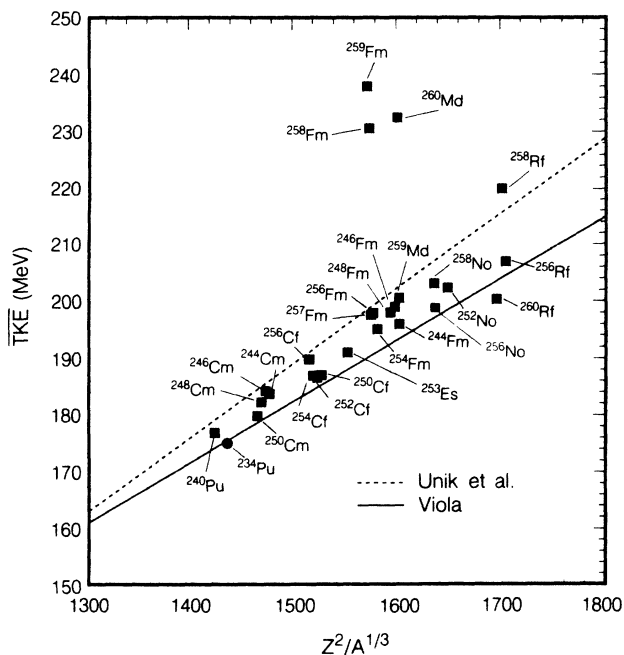


FIG. 2.  $\overline{\text{TKE}}$  vs  $Z^2/A^{1/3}$ . Solid line is linear fit of Viola (Ref. 3); dashed line is from Unik *et al.* (Ref. 4). Most measurements from solid-state detectors were based on the SKW (Ref. 5) calibration parameters. Our value for  $^{256}\text{No}$  is based on the calibration parameters of Weissenberger *et al.* (Ref. 6) which results in  $\overline{\text{TKE}}$ 's about 3–4 MeV lower. Points designated by ■ are for SF; point designated by ● is for electron-capture delayed fission.

and SF half-lives, and have confirmed the assignment of a 2.91-s, 8.448-MeV  $\alpha$  activity to  $^{256}\text{No}$  by correlation with its  $^{252}\text{Fm}$  daughter activity. From measurements of the kinetic energies of coincident fission fragments, we have derived the TKE and mass-yield distributions. We have also measured the energies of the  $\alpha$  transitions to the ground state and  $2^+$ -excited state of  $^{252}\text{Fm}$ .

## II. EXPERIMENTAL PROCEDURES

$^{256}\text{No}$  was produced at the Lawrence Berkeley Laboratory 88-Inch Cyclotron via the  $^{248}\text{Cm}(^{12}\text{C},4n)$  reaction. In initial experiments, single  $^{248}\text{Cm}_2\text{O}_3$  targets (containing either 0.66-mg/cm<sup>2</sup> or 0.49-mg/cm<sup>2</sup>  $^{248}\text{Cm}$ , 97% isotopic purity), deposited by the molecular plating method<sup>10</sup> in a 0.6-cm diameter on 2.75-mg/cm<sup>2</sup> Be foils were used. In subsequent experiments, because of the small production cross section and small fission branch for  $^{256}\text{No}$ , we used our multiple target system<sup>11</sup> with two  $^{248}\text{Cm}$  targets to maximize the production of  $^{256}\text{No}$ . When a single target was used, the beam energy was chosen so as to result in  $^{12}\text{C}^{4+}$  energies of 70–72 MeV (laboratory system) on target, close to the maximum of 71

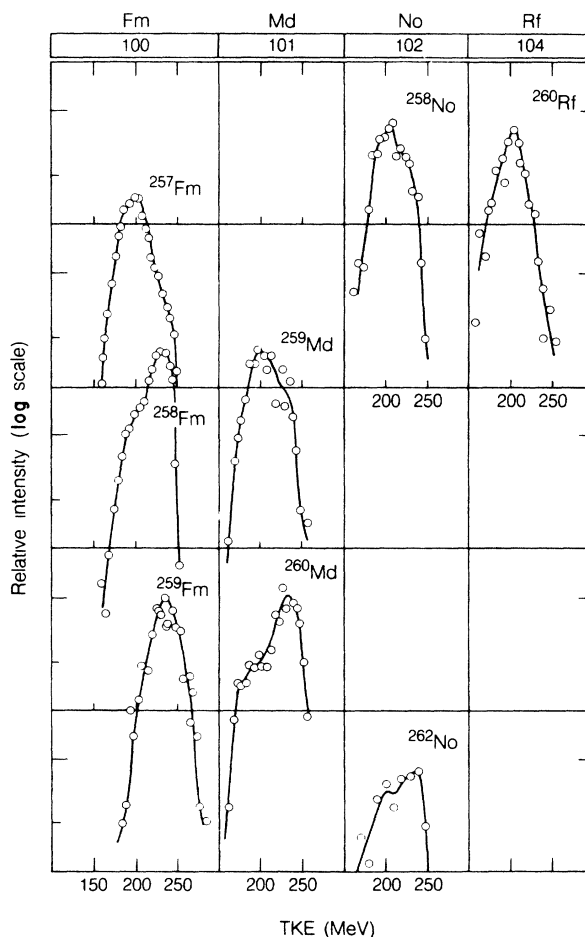


FIG. 3. Schematic of TKE distributions for SF of some heavy trans-Es isotopes (from Ref. 2).

MeV for the  $4n$  excitation function reported by Sikkeland *et al.*<sup>12</sup> The  $^{12}\text{C}^{4+}$  beam from the cyclotron passed through a 1.8-mg/cm<sup>2</sup> HAVAR entrance window, 0.2-mg/cm<sup>2</sup>  $\text{N}_2$  cooling gas, the Be target backing foil (2.75 mg/cm<sup>2</sup>), and into the first target containing 0.54 mg/cm<sup>2</sup>  $\text{Cm}_2\text{O}_3$  (0.49 mg/cm<sup>2</sup> of  $^{248}\text{Cm}$ ). When a second target was used, the beam then passed through 0.36 mg/cm<sup>2</sup> of He, the second Be target backing foil (2.08 mg/cm<sup>2</sup>), the second target containing 0.75 mg/cm<sup>2</sup>  $\text{Cm}_2\text{O}_3$  (0.66 mg/cm<sup>2</sup> of  $^{248}\text{Cm}$ ), and finally a second zone of 0.36 mg/cm<sup>2</sup> of He, before passing through a Be foil used to limit the recoil volume behind the final target so it was the same as that of the preceding target. The resulting beam energies for  $^{12}\text{C}^{4+}$  ions entering the first and second targets were calculated to be 75.8 and 70.4 MeV, respectively, in the laboratory system. The beam currents were typically about 0.8 particle  $\mu\text{A}$ .

Reaction products recoiling out of the targets were thermalized in He at a pressure of 1.2 bar and transported out of the target chamber via a He-jet gas transport system containing KCl aerosol. The aerosol-loaded helium was drawn through 1.2-mm i.d. polyvinyl chloride capillary tubing to the vacuum chamber of our horizontal rotating wheel system,<sup>13</sup> the MG, located about 10 m away. The 25.4-cm radius horizontal wheel of the MG has 80 equally spaced collection positions about its circumference. A steel ring with a 0.63-mm i.d. hole, which was covered with a  $40 \pm 15 \mu\text{g}/\text{cm}^2$  film of polypropylene, was placed in each collection position. The efficiency of the He-jet system for transporting and depositing recoiling  $^{256}\text{No}$  atoms on these films was estimated to be about 75%. This estimate was based on a comparison of Fm isotope yields from the He jet system with yields of Fm isotopes determined in separate 1-h irradiations in which recoiling products were deposited in Au catcher foils placed directly behind the target. The actinide fraction was separated from these foils and analyzed according to the procedure given by Kratz *et al.*<sup>14</sup>

The wheel was rotated at 3-s intervals so as to move the foils consecutively from the collection site into position between pairs of passivated, ion-implanted planar silicon detectors. These detectors had a depletion depth of 300 microns and an active surface area of 100 mm<sup>2</sup>. Six pairs of detectors were used to measure the kinetic energies of the fission fragments and alpha particles. The foils were changed every 20 min (5 revolutions of the wheel) in order to minimize the accumulation of any possible longer-lived activities. The source-to-detector distance of about 2.0 mm gave an efficiency for the detection of  $\alpha$  particles in a given detector of 30%. Since each detection station consisted of two detectors at 180° to each other, one above and the other below the wheel, the efficiency for the detection of  $\alpha$  particles or coincident fission fragments was about 60%. The typical  $\alpha$ -particle energy resolution was 25 keV for the top detectors and 35–40 keV for the bottom detectors because of the interposed polypropylene collection foil. Off-line  $\alpha$ -energy calibrations were obtained by measuring the known  $\alpha$  groups from  $^{212}\text{Bi}$  and  $^{212}\text{Po}$  in equilibrium with a  $^{212}\text{Pb}$  source. On-line  $\alpha$ -energy calibrations were made using Ra and Po activities produced from a small amount of Pb in the tar-

get. Sources of  $^{252}\text{Cf}$  on similar polypropylene foils were used for the energy calibration for SF fragments according to the calibration procedure of Schmitt, Kiker, and Williams<sup>5</sup> (SKW) using revised constants recently determined by Weissenberger *et al.*<sup>6</sup> This gives kinetic energies for fission fragments which are lower by 1–2 % and yields a post-neutron emission average TKE of 181.03 MeV for  $^{252}\text{Cf}$  vs 184.14 MeV from the original SKW constants. A comparison of our results for  $^{256}\text{No}$  obtained using the original SKW parameters and the Weissenberger parameters was made.

Pulses above 5 MeV triggered the storage of the signals from a given detector station. Pulses from  $\alpha$  particles between 5 and 10 MeV and fission fragments up to 200 MeV from each detector were digitized by octal analog-to-digital converters (ADC's) and stored in list mode on magnetic tape by our real-time data acquisition and graphics system (RAGS).<sup>15</sup> The timing requirement for coincident fission fragments was 2  $\mu\text{s}$ . Pulses indicating the times of rotation of the wheel and the beam intensity were also recorded.

### III. RESULTS

#### A. Half-life determination

The best value for the  $^{256}\text{No}$  half-life was obtained from analysis of the decay of the  $\alpha$  spectrum measured in the top detectors. The measured ratios of  $^{256}\text{No}$   $\alpha$  activity to  $^{214}\text{Ra}$   $\alpha$  activity ( $t_{1/2} = 2.46 \pm 0.03$  s) (Ref. 16) as a function of time,  $R(t)$ , can be used to accurately determine the half-life of  $^{256}\text{No}$  from the relation:  $\lambda_{\text{No}} = \lambda_{\text{Ra}} - d[\ln R(t)]/dt$  where  $\lambda_{\text{No}}$  and  $\lambda_{\text{Ra}}$  are the decay constants of  $^{256}\text{No}$  and  $^{214}\text{Ra}$ , respectively. This method eliminates errors due to uncertainties in detector efficiencies and possible changes during the course of the experiments. The best value of the half-life, found by performing an error-weighted least-squares fit to  $\ln[R(t)]$ , is  $2.91 \pm 0.05$  s. This value is considerably more accurate than those of  $2.9 \pm 0.5$  s,  $3.2 \pm 0.2$  s, and  $3.7 \pm 0.5$  s reported<sup>8,9</sup> previously.

A least-squares fit to the decay data for coincident SF fragments measured in the first 5 detector stations gave a half-life of  $3.0 \pm 0.2$  s, consistent with the half-life obtained for the  $\alpha$  decay. There was no evidence for longer-lived SF species.

The production cross section for  $^{256}\text{No}$  for 71-MeV  $^{12}\text{C}$  projectiles was measured to be 250 nb based on a He jet transport yield of 75% and an effective target thickness equal to the range of the No compound nucleus products of about 0.40 mg/cm<sup>2</sup>. Our cross-section value is much lower than that of about 740 nb measured by Giorso *et al.*<sup>8</sup> for 71-MeV  $^{12}\text{C}$  ions. We do not know the reason for this rather large discrepancy as they estimate their beam energies to be accurate to  $\pm 2$  MeV and their excitation function shows little change in cross section between 68 and 73 MeV. If our  $^{248}\text{Cm}$  target is much thicker due to extraneous mass then we might get too low a value although this does not appear to be the case. The measurement of absolute cross sections was not the object of this

work, but this discrepancy needs to be investigated further in experiments with thinner targets.

### B. SF branch of $^{256}\text{No}$

From a comparison of the measured SF coincidences with the number of  $^{256}\text{No}$   $\alpha$  particles detected in the bottom detectors (which more closely approximates the efficiency for measurement of SF coincidences), the SF/ $\alpha$  ratio was determined to be 0.0053 with a statistical standard deviation of 0.0003. Corrections to the number of  $^{256}\text{No}$  alphas were made for the small amount (2.7%) of  $^{214}\text{Fr}$  (produced from decay of  $^{214}\text{Ra}$ ) and for an estimated 1% of  $^{256}\text{No}$   $\alpha$  decay to other than the  $0^+$  and  $2^+$  levels of  $^{252}\text{Fm}$ . The finite size of the sources may cause the efficiency for detecting fission coincidences to be somewhat less than twice the  $\alpha$ -particle detection efficiency in the bottom detectors. Consequently, we estimate the error in the SF/ $\alpha$  ratio of 0.0053 to be  $+0.0006$  and  $-0.0003$ , which gives a partial SF half-life of  $550_{-70}^{+40}$  s.

### C. Confirmation of the assignment of the 2.9-s alpha activity to $^{256}\text{No}$

The confirmation of the assignment of a 2.9-s, 8.448-MeV  $\alpha$  activity to  $^{256}\text{No}$  was made by an indirect correlation with its  $^{252}\text{Fm}$  daughter activity ( $t_{1/2}=25.4$  h,  $E_\alpha=7.039$  MeV).<sup>17</sup> The recoil momentum of 0.134 MeV imparted to the  $^{252}\text{Fm}$  daughter by  $\alpha$  decay of  $^{256}\text{No}$  is sufficient to eject the  $^{252}\text{Fm}$  atoms from the deposited source and implant them in the top detector face. The wheel is stepped at 3-s intervals so the distribution of these  $^{252}\text{Fm}$  recoils in the successive top detectors is related to the  $^{256}\text{No}$  half-life. At the end of one series of irradiations, the  $^{252}\text{Fm}$  activity which had recoiled onto the

top detectors was measured for several days. The  $\alpha$  energy and half-life of this activity were consistent with the known values for  $^{252}\text{Fm}$  and the distribution of  $^{252}\text{Fm}$  in the top detectors was consistent with our measured value of the  $^{256}\text{No}$  half-life. The number of  $^{252}\text{Fm}$  recoils on the top detector surfaces after the bombardment indicated that  $33\pm 4\%$  of the No  $\alpha$  decays resulted in the implantation of the  $^{252}\text{Fm}$  daughter in the top detector faces. This implantation efficiency is consistent with our source-to-detector distance ( $\alpha$  efficiency) and indicates very little absorption of the recoils in the KCl of the sources and the He gas between the foils and the detector. This is the first definite assignment of the 2.9-s, 8.448-MeV  $\alpha$  activity to the decay of a No isotope with mass number 256.

Based on the consistency of the SF half-life of  $3.0\pm 0.2$  s with that of the  $^{256}\text{No}$   $\alpha$  half-life of  $2.91\pm 0.05$  s, the relative constancy of the SF/ $\alpha$  ratio from different runs at somewhat different  $^{12}\text{C}$  energies, and the absence of any indication of longer-lived SF activities, we also attribute the observed  $3.0\pm 0.2$  s SF activity to  $^{256}\text{No}$ .

### D. $^{256}\text{No}$ alpha-energy spectrum

A plot of the  $\alpha$  spectrum taken with the station two top detector from 3.15 to 6.00 s after the end of collection of the activity from a 18.8-particle  $\mu\text{Ah}$  bombardment is presented in Fig. 4. The activities in the Bi-Ra region are due to the interaction of the  $^{12}\text{C}$  beam with a small amount of Pb impurity in the target. The energy of the main peak of the  $^{256}\text{No}$  spectrum was determined by analysis of the data in the top detectors. An internal linear calibration of energy versus channel number was obtained using the known<sup>16,18</sup> alpha peaks from the decay of  $^{214}\text{Ra}$  ( $E_\alpha=7136\pm 3$  keV) and  $^{211}\text{Po}^m$  ( $E_\alpha=8885\pm 5$

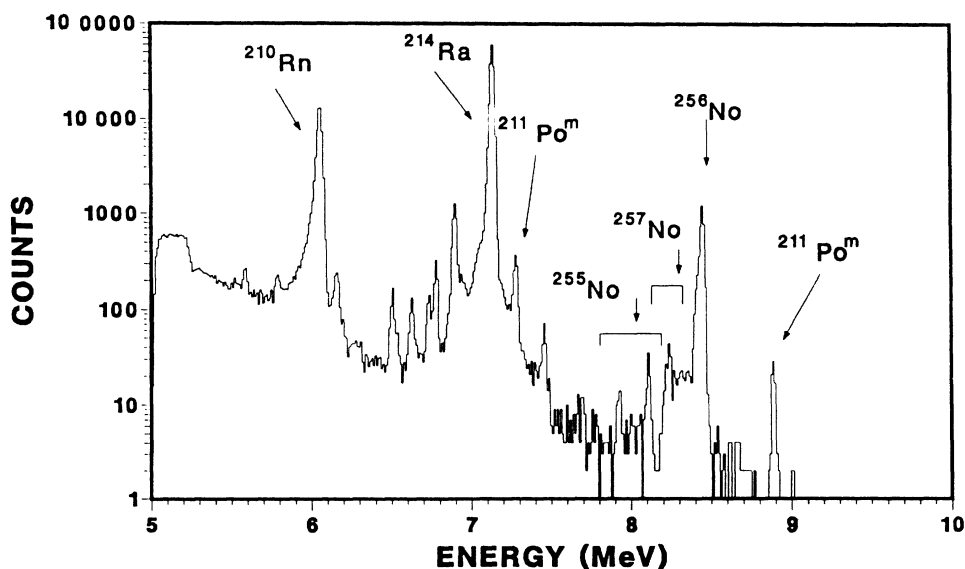


FIG. 4. Alpha-energy spectrum for  $^{256}\text{No}$  decay measured with station two top detector for a 18.8-particle  $\mu\text{Ah}$  bombardment of  $^{248}\text{Cm}$  with  $^{12}\text{C}$  ions.

keV). From this calibration an energy of  $8448 \pm 6$  keV was obtained for the  $\alpha$  particle emitted in the transition to the  $^{252}\text{Fm}$  ground state. This value is considerably more accurate than the previous best value<sup>19</sup> of  $8430 \pm 20$  keV and gives a  $Q_\alpha$  of  $8582 \pm 6$  keV. Using  $58\,449 \pm 2$  keV for the mass excess<sup>20</sup> of  $^{244}\text{Cm}$ , the  $^{248}\text{Cf}$   $Q_\alpha$  of  $6361 \pm 5$  keV,<sup>17</sup> the  $^{252}\text{Fm}$   $Q_\alpha$  of  $7153 \pm 2$  keV,<sup>17</sup> and our value for the  $^{256}\text{No}$  decay energy, we obtain a value of  $87820 \pm 8$  keV for the mass excess of  $^{256}\text{No}$ .

The rotational structure in the  $^{256}\text{No}$  spectrum was not easily visible in these experiments at high geometry (30% of  $4\pi$  sr). In order to improve the resolution, a separate irradiation in which the source-to-detector distance was adjusted so that the detectors subtended only 3.2% of  $4\pi$  sr was performed. This significantly reduced the effects of summing of  $\alpha$  particles with beta particles emitted from the source and of summing of  $\alpha$  particles from the  $^{256}\text{No}$  decay populating the  $2^+$  level of the  $^{252}\text{Fm}$  ground-state rotational band with conversion electrons from the deexcitation of this level. The  $\alpha$ -particle energy resolution measured in these experiments was 21 keV FWHM for the 7136-keV  $^{214}\text{Ra}$  peak. The  $\alpha$  peaks from the decay of  $^{256}\text{No}$  to the  $0^+$  and  $2^+$  rotational states in the  $^{252}\text{Fm}$  daughter were fit with an error weighted, non-linear least-squares procedure<sup>21</sup> as shown in Fig. 5. The peak shape parameterization used in this fit was a Gaussian function smoothly joined to an exponential tail on the low-energy side. The Gaussian width and the exponential slope for this fit were fixed at values which were determined from the  $^{214}\text{Ra}$  alpha peak in the same spectrum (see Fig. 5). Based on the energy difference between the two peaks of  $45.9 \pm 1.2$  keV, we calculate that the energy of the  $2^+$ -rotational level in  $^{252}\text{Fm}$  is 46.6 keV. We estimate the one sigma error in this value to be 5 keV to allow for the possibility of a small contribution from interfering activities in the region below the low-intensity  $\alpha$  peak. Because of the method used for energy calibration, energy differences over a small energy range can be calculated more accurately than absolute energies. Based on this measured energy difference, we calculate the energy of the  $\alpha$  group populating the  $2^+$  level to be 8.402 MeV with an estimated error of  $\pm 8$  keV. The relative intensity of this group obtained from the fitting procedure is  $13 \pm 2\%$ . The relative intensity of the  $\alpha$  branch of  $^{256}\text{No}$  to the  $4^+$ -rotational state in  $^{252}\text{Fm}$  is expected to be less than 1% and was obscured by  $\alpha$  particles from the decay of 26-s  $^{257}\text{No}$ , also produced in the bombardment.

#### E. Kinetic-energy and mass-yield distributions

The kinetic energies of 346 pairs of coincident fission fragments were measured. The pre-neutron-emission TKE distribution is shown in Fig. 6. The energy calibration is based on the SKW method<sup>5</sup> using the recently determined constants of Weissenberger *et al.*<sup>6</sup> This results in a TKE about 3.4 MeV lower (about 1.7 MeV lower for both the high- and low-energy fragments) than if the original SKW constants are used. An average number of neutrons emitted as a function of fragment mass,  $\bar{\nu}(M)$ , similar to that used by Balagna *et al.*<sup>1</sup> for  $^{257}\text{Fm}$ , was used to correct the measured post-neutron emission

fragment kinetic energies and derived masses to pre-neutron-emission values. Several types of Gaussian plus exponential fits to the TKE distribution were made. The best fit gave a most probable pre-neutron-emission TKE of  $195.7 \pm 2.9$  MeV with a FWHM of 42 MeV. Contrary to TKE measurements<sup>22</sup> of some heavy actinides, there is no evidence for more than one component in the TKE distribution.

The pre-neutron-emission kinetic-energy distributions for the high- and low-energy fragments from SF of  $^{256}\text{No}$  are shown in Fig. 7. A summary of the kinetic-energy measurements for  $^{256}\text{No}$  and a  $^{252}\text{Cf}$  standard measured in the same system is given in Table I, together with similar measurements<sup>1</sup> for  $^{257}\text{Fm}$ , normalized to the new constants. From the kinetic-energy coincidence data, the pre-neutron emission mass-yield distributions shown in

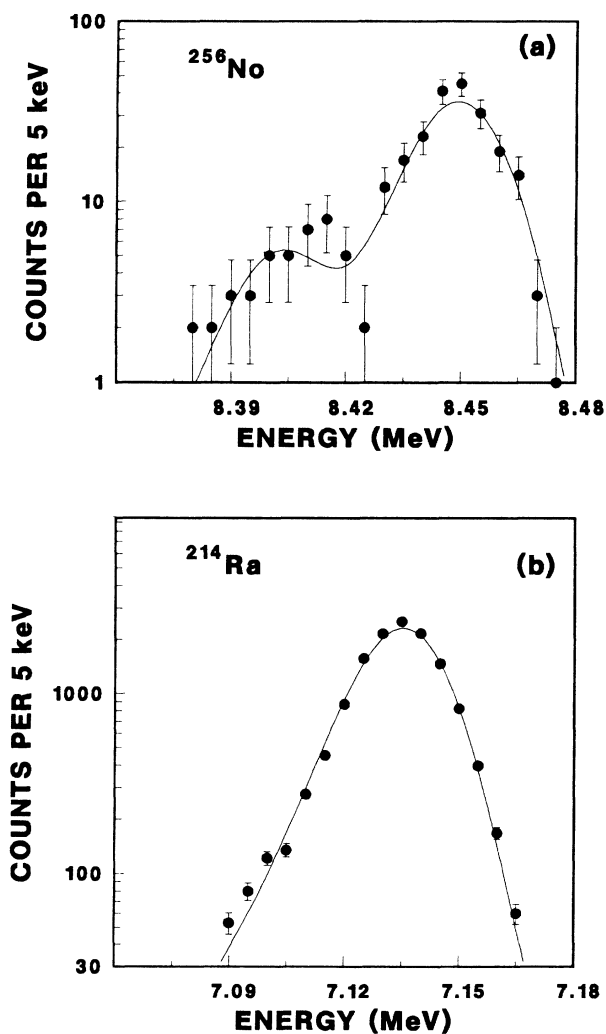


FIG. 5. (a) Fit to high resolution  $^{256}\text{No}$  spectrum showing the  $\alpha$  groups which decay to the  $0^+$  and  $2^+$  states in  $^{252}\text{Fm}$ . (b) Fit to  $^{214}\text{Ra}$  peak which was used to determine the shape parameters for  $^{256}\text{No}$  fit.

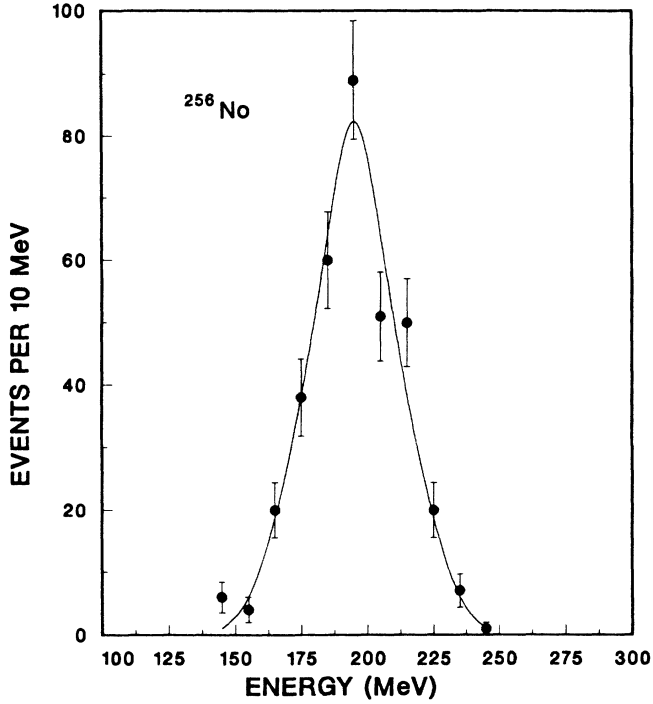


FIG. 6. Gaussian fit to pre-neutron-emission TKE distribution from SF of  $^{256}\text{No}$ .

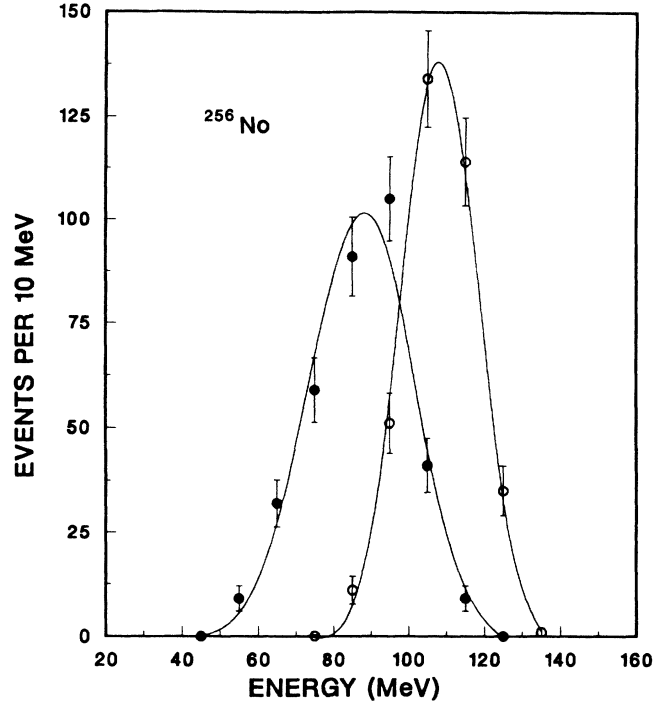


FIG. 7. Gaussian fits to pre-neutron-emission distributions for high and low kinetic-energy fragments from SF of  $^{256}\text{No}$ .

TABLE I. Properties of the measured (post-neutron-emission) and deduced initial (pre-neutron-emission) fragment kinetic-energy distributions for  $^{256}\text{No}$  (this work) and  $^{257}\text{Fm}$  (Ref. 1). Energies are given in MeV, based on the SKW calibration method (Ref. 5) with the Weissenberger constants (Ref. 6) which give 181.0 MeV for the post-neutron emission average TKE for SF of  $^{252}\text{Cf}$ .

	$^{256}\text{No}$		$^{252}\text{Cf}$		$^{257}\text{Fm}^a$	
	Pre- $n^b$	Post- $n$	Pre- $n^b$	Post- $n$	Pre- $n$	Post- $n$
Total kinetic energy						
Average	195.1	192.1	184.3	181.6	194.3	191.3
Most probable <sup>c</sup>	195.7	192.1	185.6	183.3	194.7	191.8
$\sigma$	17.7	17.1	16.0	15.7	15.3	15.5
FWHM <sup>d</sup>	41.6	40.2	37.6	36.9	36.0	36.4
Heavy fragment energy						
Average	86.7	85.7	79.6	78.6	86.8	85.9
Most probable <sup>c</sup>	86.9	86.8	79.6	78.7	86.3	85.3
$\sigma$	13.1	12.6	11.4	11.3		
FWHM <sup>d</sup>	30.8	29.6	26.8	26.6		
Light fragment energy						
Average	108.4	106.4	104.8	102.9	107.3	105.1
Most probable <sup>c</sup>	108.2	106.8	106.1	104.2	108.9	106.9
$\sigma$	9.3	9.4	9.7	9.6		
FWHM <sup>d</sup>	21.9	22.1	22.8	22.6		

<sup>a</sup>The kinetic energies for SF of  $^{257}\text{Fm}$  from Ref. 1 have been normalized to the Weissenberger constants for comparison with  $^{256}\text{No}$ .

<sup>b</sup>These were deduced from the measured post-neutron data using the procedure described in the text.

<sup>c</sup>Standard deviation of the most probable values from the Gaussian fits is about 1.5%.

<sup>d</sup>Full width at half maximum, calculated from  $2.35\sigma$  for Gaussian fit to the top half of the peak.

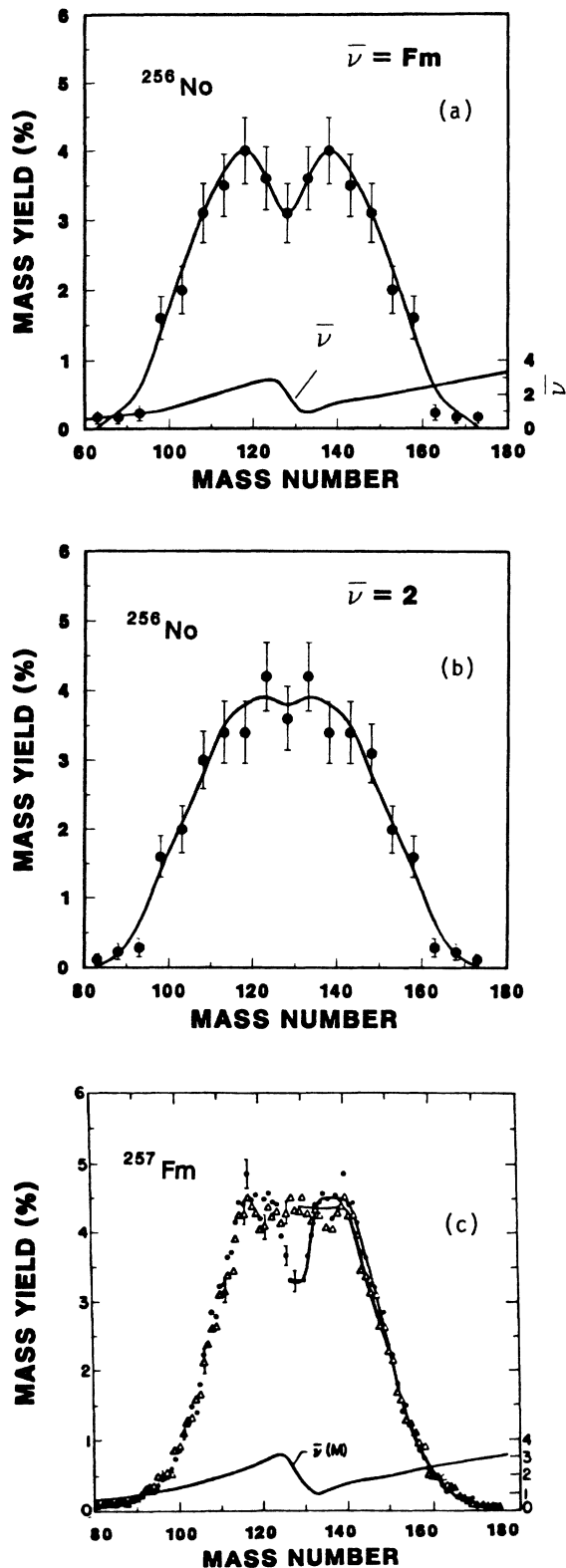


FIG. 8. Pre-neutron-emission mass-yield curves for  $^{256}\text{No}$  (346 events) obtained using (a) a  $\bar{\nu}(M)$  function similar to that used by Balagna *et al.* (Ref. 1) for  $^{257}\text{Fm}$  with  $\bar{\nu}_T = 3.77$ , and (b) a constant  $\bar{\nu}(M) = 2$ . (Curves are added only as a visual aid.) (c) Pre-neutron-emission mass-yield curves for  $^{257}\text{Fm}$  (17,951 events) from Ref. 1.

Fig. 8(a) and 8(b) have been derived. The mass-yield data are normalized to 200% fragment yield and expressed as mass yield (%) per mass number. If a saw-toothed  $\bar{\nu}(M)$  distribution similar to that measured<sup>23</sup> for  $^{252}\text{Cf}$  and used for  $^{257}\text{Fm}$  with the average number of neutrons per fission,  $\bar{\nu}_T$ , normalized to 3.77 (the measured value<sup>24</sup> for  $^{257}\text{Fm}$ ) is used, a mass-yield distribution with a small decrease in yields near symmetry results as shown in Fig. 8(a). The distribution is very broad with a FWHM of about 50 mass units. The mass-yield distribution ob-

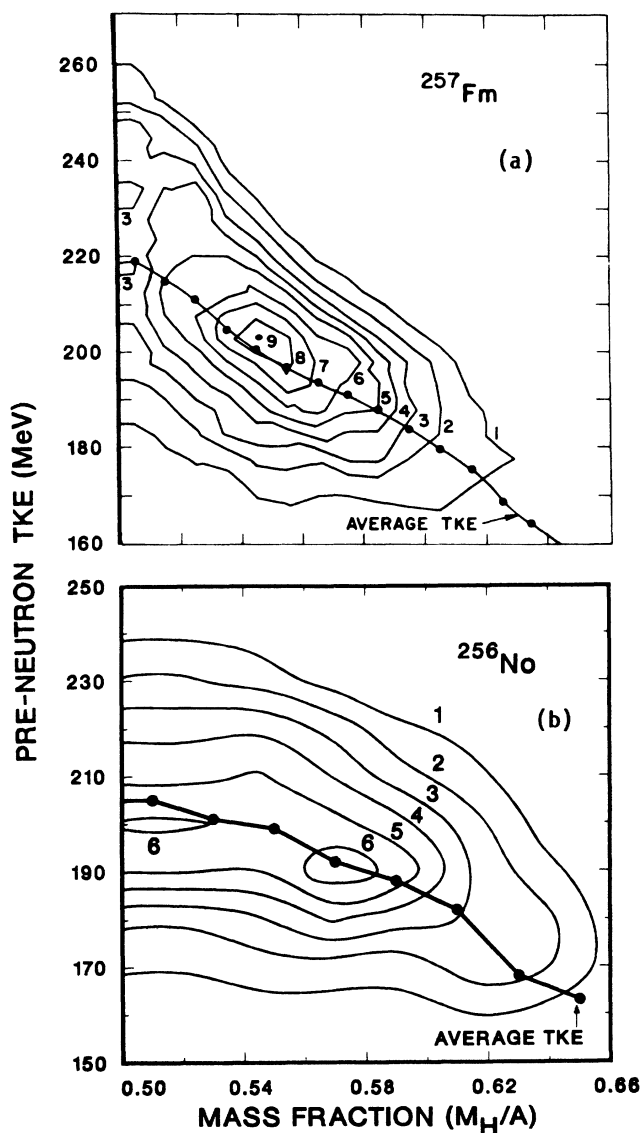


FIG. 9. Contour diagram for fission yield as a function of pre-neutron-emission TKE and mass fraction. (a)  $^{257}\text{Fm}$ . Contours are lines of relative numbers of events based on data groupings 5 MeV  $\times$  0.01 units of mass fraction; (b)  $^{256}\text{No}$ . The contours indicate equal numbers of events based on data groupings 20 MeV  $\times$  0.04 units of mass fraction. Contours labeled 1–6 represent 10 through 60 events, respectively.

tained with a flat  $\bar{\nu}(M)=2$  function results in a much smaller decrease in yields for near symmetric mass division and is shown in Fig. 8(b) for comparison. The peak-to-valley ratio for the mass distribution of the  $^{252}\text{Cf}$  standard measured in our system is about 5 to 1, whereas it was about 10 to 1 for the system in Ref. 1 and the FWHM of our TKE distribution was about 37 MeV compared to 30 MeV for  $^{252}\text{Cf}$  in Ref. 1.

A contour plot of the pre-neutron-emission TKE distributions as a function of mass fraction for SF of  $^{256}\text{No}$  is shown in Fig. 9(b). The contours are lines of relative numbers of events in 6 equal increments of 10 events each. Because only 346 coincident pairs of fragments were measured, rather coarse data groupings of  $10 \text{ MeV} \times 0.04$  units of mass fraction were used, and a smoothing procedure was utilized to obtain intermediate values and help define the contours. The average TKE over intervals of 0.02 units of mass fraction (5.1 mass units) is also shown in Fig. 9(b). A similar type of plot for  $^{257}\text{Fm}$  is shown in Fig. 9(a) for comparison; in this case, nearly 18000 events were measured<sup>1</sup> so the statistics are much better and the smaller data groupings of  $5 \text{ MeV} \times 0.01$  units of mass fraction give significantly better resolution.

#### IV. DISCUSSION

We have added our mass-yield distribution for SF of  $^{256}\text{No}$  to the schematic representations shown in Fig. 1 for the SF of trans-Bk isotopes. The mass distribution for  $^{252}\text{No}$  is asymmetric,<sup>25</sup> similar to those observed for Fm isotopes with  $N \leq 156$  and its TKE appears "normal" in Fig. 2. The progression from asymmetric to symmetric mass division for the No isotopes appears to be similar to that for the Fm isotopes, but based on our measurements for  $^{256}\text{No}$ , it appears that the transition occurs at  $N = 154$  in the No isotopes ( $^{254}\text{No}$  with  $N = 152$  has not yet been measured), three neutrons fewer than in the Fm isotopes where the transition occurs at  $N = 157$ . It is of interest to compare the SF properties of  $^{256}\text{No}$  with  $^{257}\text{Fm}$ , the transition nucleus between asymmetric and symmetric mass division in the Fm isotopes. From Fig. 8, it can be seen that the mass-yield curve for  $^{256}\text{No}$  is very similar to that for  $^{257}\text{Fm}$ . The major difference is that the FWHM of the  $^{256}\text{No}$  mass distribution is about 50 mass units while that of  $^{257}\text{Fm}$  is only about 44 mass units. This may be due in part to our relatively poorer resolution resulting from nonuniformities in the thickness ( $40 \pm 15 \mu\text{g}/\text{cm}^2$ ) of the polypropylene foils and our source-to-detector distance of only about 2 mm and from the necessity for averaging over larger mass and energy intervals because only 346 coincident events were measured. Both nuclides show nearly the same peak-to-valley ratios of 1 to 1.4, depending on the neutron correction used.

The most probable pre-neutron emission TKE for  $^{256}\text{No}$  is  $195.7 \pm 2.9 \text{ MeV}$  with a FWHM of 42 MeV. This TKE appears to be rather low on the plot of TKE vs  $Z^2/A^{1/3}$  shown in Fig. 2. It is nearly identical to that of 194.7 MeV (Table I) with a FWHM of 36 MeV measured<sup>1</sup> for  $^{257}\text{Fm}$  and similar to that of 202.4 MeV (199 MeV corrected to the Weissenberger constants) measured for  $^{252}\text{No}$  by Bemis *et al.*<sup>25</sup> It is somewhat lower than that

of 204 MeV measured for  $^{258}\text{No}$  by Hulet *et al.*<sup>22</sup> who find evidence for a very low-intensity (5%) higher-energy component around 232 MeV, shown schematically in Fig. 3. They have also decomposed<sup>22</sup> the distributions for  $^{258}\text{Fm}$ ,  $^{259}\text{Md}$ , and  $^{260}\text{Md}$  into two Gaussian distributions of varying intensities, one centered around 200 MeV and the other around 235 MeV. They have called this "bimodal" symmetric fission postulating that one symmetric mode leads to nearly spherical fragments with anomalously high TKE due to the higher Coulomb repulsion and the other to elongated fragments with lower TKE. The high-energy mode may be associated with the new, second valley to fission leading to near-spherical or compact shapes, and thus higher total kinetic energies, shown in recent calculations of Ćwiok *et al.*<sup>26</sup> and Möller *et al.*<sup>27,28</sup>. The "old" valley leads to elongated fragments and lower kinetic energies. The TKE distribution for  $^{262}\text{No}$  has been similarly decomposed by Lougheed *et al.*<sup>7</sup> into two Gaussians centered at 237 MeV (65%) and 200 MeV (35%), respectively. Our TKE for  $^{256}\text{No}$  is dramatically lower than that for  $^{262}\text{No}$ . It shows no evidence for a high-energy component (Fig. 6) and is fit best with a single Gaussian. However, the TKE distribution for  $^{257}\text{Fm}$  (Fig. 3) does show a "bulge" on the high-energy side which is more evident in the contour plot shown in Fig. 9(a). The variance of the TKE for symmetric mass division is extremely large, indicating shapes ranging from near spherical with TKE's approaching the  $Q$  value, to deformed shapes with low TKE. This appears to be "multimodal," rather than just bimodal, symmetric fission. Indeed, calculations of Paskevich<sup>29</sup> for  $^{264}\text{Fm}$  have shown three valleys on the potential-energy surface for symmetric fission in the region of the scission point. Our contour plot for  $^{256}\text{No}$  [Fig. 9(b)] appears to be qualitatively different from that for  $^{257}\text{Fm}$ , inasmuch as there is a rather large region of nearly constant TKE extending from symmetric mass division to a mass fraction of about 0.58 ( $A = 148$ ). The average TKE for symmetric mass division for  $^{257}\text{Fm}$  is about 220 MeV compared to only about 205 MeV for  $^{256}\text{No}$  although the TKE's are nearly the same for both nuclides for very asymmetric mass division, i.e., for  $M_H/A \gtrsim 0.56$ .

Our data imply that the fragments from symmetric division of  $^{256}\text{No}$  are more deformed and thus have lower TKE's than those from symmetric fission of  $^{257}\text{Fm}$ .  $^{256}\text{No}$ , with 102 protons and only 154 neutrons, apparently is not influenced as much by spherical shells in the fragments as is the case for  $^{257}\text{Fm}$  and heavier Fm isotopes in which symmetric mass division approaches the doubly magic  $Z = 50, N = 82$  configuration. In  $^{256}\text{No}$ , we see both symmetric and asymmetric mass division with about the same TKE, consistent with TKE values extrapolated from lighter actinides as shown in Fig. 2. The extremely broad mass distribution with a FWHM of about 50 mass units measured for  $^{256}\text{No}$  is reminiscent of the liquid-drop type fission observed in the preactinide region and in the higher-energy fission of lighter actinides in which the extra energy is sufficient to overcome the shell effects which tend to stabilize asymmetric division. It is perhaps somewhat surprising that there is so little indication of any high-energy, mass-symmetric fission in  $^{256}\text{No}$ ,



but this is consistent with one  $Z = 50$  fragment with too few neutrons ( $N$  less than 78) to be spherical and a complementary fragment with  $Z = 52$  and  $N = 76$ , also not likely to be spherical. In the Fm isotopes, the high-energy, narrowly symmetric mode does not become most probable until <sup>258</sup>Fm whose symmetric mass division can give two  $Z = 50$  fragments with  $N = 79$ . Again, we see how sensitive the fission properties of these heavy actinide isotopes are to changes of only a nucleon or two, and the stringent demands that such dramatic and abrupt changes place on the theoretical models.

#### ACKNOWLEDGMENTS

The authors are indebted to the Division of Chemical Sciences, Office of Basic Energy Sciences, U.S. Department of Energy, for making the <sup>248</sup>Cm available through the transplutonium production facilities at the Oak Ridge National Laboratory. We wish to thank the staff and crew of the Lawrence Berkeley Laboratory 88-Inch Cyclotron for providing the <sup>12</sup>C beams. This work was supported in part by the U.S. Department of Energy under Contract No. DE-AC03-76SF00098.

\*Present address: Department of Nuclear Engineering, National Tsing Hua University, Hsinchu, Taiwan, Republic of China.

- <sup>1</sup>J. P. Balagna, G. P. Ford, D. C. Hoffman, and J. D. Knight, *Phys. Rev. Lett.* **26**, 145 (1971).
- <sup>2</sup>D. C. Hoffman, *Proceedings of the Conference on 50 Years With Nuclear Fission, National Institute of Standards and Technology, Gaithersburg, 1989* (American Nuclear Society, LaGrange Park, 1989), Vol. I, p. 83; Lawrence Berkeley Laboratory Report No. LBL-27093.
- <sup>3</sup>V. E. Viola, *Nucl. Data* **A1**, 391 (1966).
- <sup>4</sup>J. P. Unik, J. E. Gindler, L. E. Glendenin, K. F. Flynn, A. Gorski, and R. K. Sjolom *Proceedings of the Third International IAEA Symposium on the Physics and Chemistry of Fission, Rochester, 1973* (IAEA, Vienna, 1974), Vol. II, p. 33.
- <sup>5</sup>H. W. Schmitt, W. E. Kiker, and C. W. Williams, *Phys. Rev.* **137**, B837 (1965).
- <sup>6</sup>E. Weissenberger, P. Geltenbort, A. Oed, F. Gönnerwein, and H. Faust, *Nucl. Instrum. Methods A* **248**, 506 (1986).
- <sup>7</sup>R. W. Loughheed, E. K. Hulet, K. J. Moody, J. F. Wild, R. J. Dougan, D. C. Hoffman, C. M. Gannett, R. A. Henderson, and D. M. Lee, *Spontaneous Fission and Decay Properties of <sup>261,262</sup>Lr and the New Isotope, <sup>262</sup>No*, *Proceeding of the 3rd Chemistry Congress of North America, Toronto, Canada, 1988* (unpublished); Nuclear Chemistry Division FY-1988 Annual Report, Lawrence Livermore National Laboratory, UCAR-10062-88, 1988 (unpublished), p. 135.
- <sup>8</sup>A. Ghiorso, T. Sikkeland, and M. J. Nurmi, *Phys. Rev. Lett.* **18**, 401 (1967).
- <sup>9</sup>G. N. Flerov, A. G. Demin, V. A. Druin, Yu. V. Lobanov, V. L. Mikheev, S. M. Polikanov, and V. A. Shchegolev, *Yad. Fiz.* **7**, 239 (1968) [*Sov. J. Nucl. Phys.* **7**, 168 (1968)].
- <sup>10</sup>D. Aumann and G. Mullen, *Nucl. Instrum. Methods.* **115**, 75 (1974).
- <sup>11</sup>H. L. Hall, M. J. Nurmi, and D. C. Hoffman, *Nucl. Instrum. Methods A* **276**, 649 (1989).
- <sup>12</sup>T. Sikkeland, A. Ghiorso, and M. J. Nurmi, *Phys. Rev.* **172**, 1232 (1968).
- <sup>13</sup>D. C. Hoffman, D. Lee, A. Ghiorso, M. Nurmi, and K. Aleklett, *Phys. Rev. C* **22**, 1581 (1980).
- <sup>14</sup>J. V. Kratz, H. P. Zimmerman, U. W. Scherer, M. Schädel, W. Brüche, K. E. Gregorich, C. M. Gannett, H. L. Hall, R. A. Henderson, D. M. Lee, J. D. Leyba, M. J. Nurmi, D. C. Hoffman, H. Gäggeler, D. Jost, U. Baltensperger, Ya Nai-Qi, A. Türler, Ch. Lienert, Gesellschaft für Schwerionenforschung Darmstadt Report GSI-89-37, 1989.
- <sup>15</sup>R. G. Leres, Lawrence Berkeley Laboratory Report LBL-24808, 1987 (unpublished).
- <sup>16</sup>J. K. Tuli, R. R. Kinsey, and M. J. Martin, *Nucl. Data Sheets* **55**, 708 (1988).
- <sup>17</sup>I. Ahmad and J. L. Lerner, *Nucl. Phys.* **A413**, 423 (1984).
- <sup>18</sup>J. D. Bowman, E. K. Hyde, and R. E. Eppley, Lawrence Berkeley Laboratory, Nuclear Chemistry Division 1972 Annual Report, LBL-1666, 1973 (unpublished), p. 4.
- <sup>19</sup>M. R. Schmorak, *Nucl. Data Sheets* **32**, 87 (1981).
- <sup>20</sup>A. H. Wapstra and G. Audi, *Nucl. Phys.* **A432**, 1 (1985).
- <sup>21</sup>K. E. Gregorich, Lawrence Berkeley Laboratory Report LBL-20192, 1985 (unpublished), p. 54.
- <sup>22</sup>E. K. Hulet, J. F. Wild, R. J. Dougan, R. W. Loughheed, J. H. Landrum, A. D. Dougan, P. A. Baisden, C. M. Henderson, R. J. Dupzyk, R. L. Hahn, M. Schädel, K. Sümmerer, and G. R. Bethune, *Phys. Rev. C* **40**, 770 (1989).
- <sup>23</sup>H. R. Bowman, J. C. D. Milton, S. G. Thompson, and W. J. Swiatecki, *Phys. Rev.* **129**, 2133 (1963).
- <sup>24</sup>J. P. Balagna, J. A. Farrell, G. P. Ford, A. Hemmendinger, D. C. Hoffman, L. R. Veaser, and J. B. Wilhelmy, *Proceedings of the Third International IAEA Symposium on the Physics and Chemistry of Fission, Rochester, 1973* (IAEA, Vienna, 1974), Vol. II, p. 191.
- <sup>25</sup>C. E. Bemis, Jr., R. L. Ferguson, F. Plasil, R. J. Silva, F. Pleasanton, and R. L. Hahn, *Phys. Rev. C* **15**, 705 (1977).
- <sup>26</sup>S. Ćwiok, P. Rozmej, A. Sobiczewski, and Z. Patyk, *Nucl. Phys.* **A491**, 281 (1989).
- <sup>27</sup>P. Möller, J. R. Nix, and W. J. Swiatecki, *Nucl. Phys.* **A469**, 1 (1987).
- <sup>28</sup>P. Möller, J. R. Nix, and W. J. Swiatecki, *Nucl. Phys.* **A492**, 349 (1989).
- <sup>29</sup>V. V. Pashkevich, *Nucl. Phys.* **A477**, 1 (1988).